3. Electrocatalytic Chelation of $[FeCp^*(\eta^1\text{-dtc})(CO)_2]$ by 0.1 Equiv of $[FeCp_2]^+PF_6^-$ in CH_2Cl_2. A 0.1-g sample of complex **1b** (0.2725 mmol) and 9 mg of $[FeCp_2]^+PF_6^-$ were stirred in CH_2Cl_2 in the dark, under argon for 10 min. The solvent was then evaporated, and the crude product extracted with dry ether, which was then evaporated. The same workup as in 1 gave 12% yield for complex **2b** and 68% yield for the starting material **1b**.

4. Chelation of $[FeCp^*(\eta^1\text{-dtc})(CO)_2]$ by 1 Equiv of $[FeCp_2]^+BF_4^-$ in the Presence of $[nBu_4N^+][BF_4^-]$. A 0.054-g sample of complex **1b** (0.147 mmol), 0.040 g of $[FeCp_2]^+BF_4^-$ (0.147 mmol), and 2 g of $[nBu_4N^+][BF_4^-]$ (6.079 mmol) were stirred at room temperature, in the dark, under argon in 10 mL of THF for 10 min. A red-brown color immediately appeared. Evaporation of the solvent gave an orange-brown powder that showed the same ESR spectrum as the product obtained by electrosynthesis, indicating the structure $[FeCp^*(\eta^2\text{-dtc})(THF)]^+BF_4^-$ (ESR (solid-state sample, 10 K) $g_1 = 2.323$, $g_2 = 2.050$, $g_3 = 2.004$).

5. $[FeCp^*(\eta^2\text{-dtc})(PPh_3)]^+PF_6^-$ ($4b^+PF_6^-$). A 0.300-g sample of complex **1b** (0.817 mmol) in 10 mL of CH_3COCH_3 was stirred with 0.214 g (0.817 mmol) of triphenylphosphine and 0.270 g (0.817 mmol) of $[FeCp_2]^+PF_6^-$ for 30 min at room temperature under argon. The red-purple solution was then filtered through a Celite column (1-cm height) and washed with CH_3CN. Addition of absolute ethanol was followed by a recrystallization by slow evaporation of CH_3CN without warming. Purple microcrystalline powder of complex $4b^+PF_6^-$ (0.507 g, 86% yield) was recovered and identified by comparison with an authentic sample.

6. Bulk Electrolysis of 1b. Electrochemical 1e oxidation of 0.369 g of **1b** (1 mmol) was performed in 30 mL of THF-0.3 M $[nBu_4N^+][BF_4^-]$, in a divided cell. The anodic compartment was equipped with a gold grid (5 cm^2) as the working electrode and a SCE + THF, 0.3 M $[nBu_4N^+][BF_4^-]$ salt bridge as the reference electrode. The cathodic reaction was reduction of 4-chlorobenzonitrile at a platinum gauze electrode (5 cm^2). Oxidation was performed at 1 V vs SCE. After 1 F/mol was passed, cyclic voltammetry showed that 99% of the starting material had disappeared, to lead to the observation of the CV traces observed in microelectrolytic conditions in Figure 4. The homogeneous red-brown solution thus obtained was pumped off to dryness, to afford a solid residue (90% $[nBu_4N^+][BF_4^-]$, 10% of electrolysis product, which was characterized by comparison with an authentic sample).

Acknowledgment. Helpful experimental assistance by N. Ardoin (Université de Bordeaux I) and early work by D. Catheline (Université de Rennes I) are gratefully acknowledged. We thank the "Région Aquitaine", the CNRS (URA 35, 110, and 415), the "Université de Bordeaux I", and the "Ecole Normale Supérieure" for financial support.

Registry No. **1a**, 75900-10-6; **1b**, 89875-07-0; **2a**, 12128-65-3; **2b**, 84541-24-2; $2b^+PF_6^-$, 119366-46-0; **3a**, 11077-24-0; **3b**, 1282-37-7; **3c**, 98092-06-9; $4b^+PF_6^-$, 118228-79-8; $5b^+BF_4^-$, 124945-07-9.

(Dithiocarbamato)iron(II) Complexes: Photochemical Chelation and Ligand Exchange, Comparison with Electron-Transfer Processes, and X-ray Crystal Structures of $Fe(\eta^5\text{-}C_5Me_5)(\eta^1\text{-}SC(S)NMe_2)(CO)_2$ and $Fe(\eta^5\text{-}C_5Me_5)(\eta^2\text{-}S_2CNMe_2)(PPh_3)$

Marie-Hélène Desbois,[†] Christine M. Nunn,[‡] Alan H. Cowley,*[,‡] and Didier Astruc*[,†]

Laboratoire de Chimie Organique et Organométallique, UA CNRS No. 35, Université de Bordeaux I, 351, Cours de la Libération, 33405 Talence Cédex, France, and Department of Chemistry, College of Natural Sciences, The University of Texas, Austin, Texas 78712-1167

Received June 15, 1989

The X-ray crystal structure of $FeCp^*(\eta^1\text{-dtc})(CO)_2$ (**1**, $Cp^* = \eta^5\text{-}C_5Me_5$, $dtc = S_2CNMe_2$) confirms that the dithiocarbamate ligand is bound to iron in a monodentate mode. The photochemical chelation of **1** is carried out in dichloromethane using visible light and quantitatively gives the chelate $FeCp^*(\eta^2\text{-dtc})(CO)$ (**2**) and CO. This reaction is the best route to **2** and compares with the electron-transfer chain (ETC) processes **1** → **2** catalyzed by either oxidizing or reducing agents. The photolytic reaction, which can be carried out by monochromatic (330 nm) irradiation and monitored by visible spectroscopy, gives two isosbestic points at 394 and 432 nm. The quantum yield ($\Phi \simeq 0.6$) does not vary greatly with the polarity of the solvents, which indicates that this process is stoichiometric:photolysis of **2** in ether in the presence of **1** equiv of PPh_3 using visible light gives $FeCp^*(\eta^2\text{-dtc})(PPh_3)$ (**3**) in 80% yield and CO. This reaction compares with the stoichiometric one-electron oxidation of **1** or **2** giving 3^+ in the presence of PPh_3, followed by the one-electron reduction of 3^+ to **3**. Both complexes **1** and **3** crystallize in a triclinic system. **1**: $a = 8.582$ (2) Å, $b = 9.046$ (4) Å, $c = 12.377$ (7) Å, $\alpha = 97.05$ (4)°, $\beta = 96.84$ (3)°, $\gamma = 111.99$ (3)°, space group $P\bar{1}$, $Z = 2$, $V = 869.9$ Å^3, $\rho_{calcd} = 1.40$ g/cm^3, $R = 0.058$, $R_w = 0.091$ based on 3232 reflections with $F_o > 3\sigma(F_o)$. **3**: $a = 11.142$ (4) Å, $b = 14.958$ (4) Å, $c = 10.382$ (4) Å, $\alpha = 98.22$ (2)°, $\beta = 115.22$ (3)°, $\gamma = 102.62$ (3)°, space group $P\bar{1}$, $Z = 2$, $V = 1471.9$ Å^3, $\rho_{calcd} = 1.29$ g/cm^3, $R = 0.056$, $R_w = 0.070$ based on 4315 reflections with $F_o > 3\sigma(F_o)$. The X-ray crystal structure of **3** shows the bulk around iron, responsible for the stability of the radical 3^+.

Introduction

Inorganic dithiocarbamate (dtc) complexes are well-known,[1] but complexes containing both a dithiocarbamate and a Cp* ligand offer the opportunity of studying mixed inorganic-organometallic behavior. For instance, the chelation of $FeCp^*(\eta^1\text{-dtc})(CO)_2$ (**1**)[2] to $FeCp^*(\eta^2\text{-dtc})(CO)$ (**2**, eq 1) is the first reaction shown to be electrocatalyzed

[†] Université de Bordeaux I.
[‡] The University of Texas.

(1) (a) Fackler, J. P. *Adv. Chem. Ser.* **1976**, *150*, 394. (b) Thorn, G. D.; Ludwig, R. A. *The Dithiocarbamates and Related Compounds*; Elsevier: Amsterdam, 1962. (c) Livingstone, S. E. *Q. Rev. Chem. Soc.* **1965**, *19*, 416. (d) Eisenberg, R. *Prog. Inorg. Chem.* **1970**, *12*, 295. (e) Coucouvanis, D. *Prog. Inorg. Chem.* **1970**, *11*, 233. (f) Willemse, J.; Gras, J. A.; Steggarda, J. J.; Kiegzers, C. P. *Struct. Bonding (Berlin)* **1976**, *28*, 83.

0276-7333/90/2309-0640$02.50/0

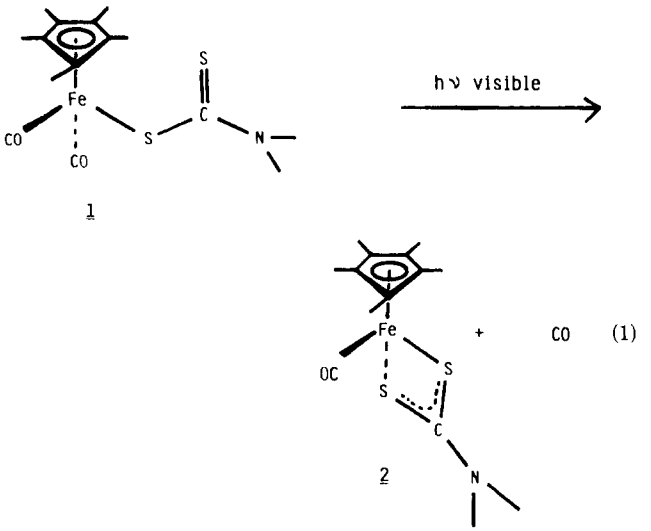

by either an oxidizing[3] or a reducing agent.[4] This property is due to the ability of the dtc ligand to stabilize various oxidation states.[1] However, relatively few monodentate complexes are known,[5] although bidentate dtc complexes are among the most numerous in the inorganic field. However, the chelation 1 → 2 proceeds with great difficulty under thermal conditions (5% yield, 100 °C).[2] On the contrary, the electron-transfer chain (ETC) catalyzed reaction proceeds rapidly at 20 °C, but in yields that are limited to 50% using oxidizing initiation and to 67% using reducing initiation.[3,4] The side reactions of the radicals, which are the intermediates in both electrocatalytic cycles, are indeed the major problem concerning the efficiency of this technique.[6] Since we wished to analyze in detail the features of these electrocatalytic processes, it was also advisable to study the photolytic reactions. The resulting information led us to exercise more care for the electrocatalytic experiments and also indicated whether a photoelectrocatalytic process should be envisaged. Determining the X-ray crystal structure of the starting compound is useful for establishing firm conclusions concerning the monohapticity of the dtc ligand. Determining that of the final photochemical product brings about an insight on the problem of the bulk around the iron center.

In this paper, we detail these photochemical and X-ray crystal structures studies and we compare the photochemical and ET reactions. The photolytic conversion of 1 to 2 was first noted in the course of electrocatalytic studies and briefly mentioned in the preceding article.[3b]

Results

Photochemistry of 1 and 2. The photolysis of 1 using visible light gives 2 cleanly in various solvents. On a millimole scale, the reaction in dichloromethane gives a 94% yield of isolated product (eq 2).

$$\underset{1}{FeCp^*(CO)_2(\eta^1\text{-}SC(S)NMe_2)} \xrightarrow[CH_2Cl_2]{h\nu\ (vis)} \underset{2}{FeCp^*(CO)(\eta^2\text{-}S_2CNMe_2)} + CO \quad (2)$$

The reaction (monitored by UV–visible spectroscopy) used monochromatic irradiation (330 nm). The progression of spectra along with the exposure time is shown on Figure 1, which shows two isosbestic points as in all the solvents used (Table I).

The characteristics of 1 and 2 are (for example, in CH_2Cl_2) λ = 394 nm, ϵ = 1777 L mol^{-1} cm^{-1} (1) and λ = 452 nm, ϵ = 934 L mol^{-1} cm^{-1} (2). A blue shift is found upon variation of the solvents from non polar to polar (Table II). The quantum yield[7] is $\phi \simeq 0.6$ and does not

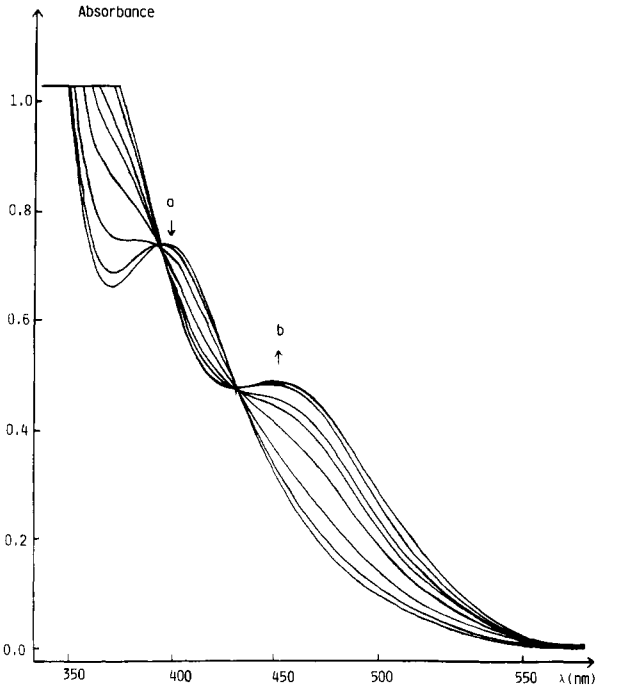

Figure 1. Substitution of the CO ligand by the free sulfur of the dithiocarbamate ligand in 1 (in CH_2Cl_2, monitored at 25 °C by visible spectroscopy) by exposure to monochromatic light (λ = 330 nm). Arrows indicate the way of evolution: (a) disappearance of 1; (b) appearance of 2.

Table I. Isosbestic Points Obtained in Different Solvents (Figure 1)

isosbestic points	CH_2Cl_2	CH_3CN	CCl_4
λ_1, nm	388	388	408
λ_2, nm	439	436	444

Table II. Variation of λ_{max} with the Polarity of the Solvent (25 °C)

	pentane	CCl_4	ether	THF	CH_2Cl_2	CH_3CN	CH_3OH
λ, nm	406	404	402	398	394	388	380
ϵ, L mol^{-1} cm^{-1}	1736	1858	1782	1921	1777	1789	1798

Table III. Variation of the Quantum Yield with the Solvent and the Wavelength of Excitation (nm)

	CH_2Cl_2		CH_3CN
	λ_{exc} = 330	λ_{exc} = 366	λ_{exc} = 366
ϕ	0.62	0.56	0.54
$t_{1/2}$, min	5.6	1.6	4.9

(2) (a) Román, E.; Catheline, D.; Astruc, D. *J. Organomet. Chem.* **1982**, *236*, 229. (b) Catheline, D.; Román, E.; Astruc, D. *Inorg. Chem.* **1984**, *23*, 4508.

(3) (a) Amatore, C.; Verpeaux, J.-N.; Madonik, A. M.; Desbois, M.-H.; Astruc, D. *J. Chem. Soc. Chem. Commun.* **1988**, 200. (b) Verpeaux, J.-N.; Desbois, M.-H.; Madonik, A. M.; Amatore, C.; Astruc, D. *Organometallics*, preceding paper in this issue.

(4) Desbois, M.-H.; Astruc, D. Submitted for publication in *J. Chem. Soc., Chem. Commun.*

(5) For synthesis of and studies on 18-electron Fe(Cp)(dithiocarbamate) complexes, see: (a) O'Connor, C.; Gilbert, J. D.; Wilkinson, G. *J. Chem. Soc. A* **1969**, 84. (b) Cotton, F. A.; Mc Cleverty, J. A. *Inorg. Chem.* **1964**, *5*, 1398. (c) Román, E.; Catheline, D.; Astruc, D.; Batail, P.; Ouahab, L.; Varret, F. *J. Chem. Soc., Chem. Commun.* **1982**, 129. (d) See also ref 2.

(6) (a) Bunnett, J. F. *Acc. Chem. Res.* **1988**, *11*, 413. (b) Savéant, J.-M. *Acc. Chem. Res.* **1980**, *13*, 323. (c) Astruc, D. *Angew. Chem., Int. Ed. Engl.* **1988**, *27*, 643.

Table IV. Crystallographic Data (Graphite Monochromatized Mo Kα Radiation, λ = 0.71073 Å) for the X-ray Structure Determination of Complexes 1 and 3[a]

formula	$C_{15}H_{21}FeNO_2S_2$	$C_{31}H_{36}FeNPS_2$
mol wt	367.32	573.59
cryst color	red	black
cryst size, mm^3	0.35 × 0.40 × 0.60	0.25 × 0.30 × 0.40
cryst habit	prism	prism
cryst syst	triclinic	triclinic
space group	$P\bar{1}$ (no. 2)	$P\bar{1}$ (no. 2)
a, Å	8.582 (2)	11.142 (4)
b, Å	9.046 (4)	14.958 (4)
c, Å	12.377 (7)	10.382 (4)
α, deg	97.05 (4)	98.22 (2)
β, deg	96.84 (3)	115.22 (3)
γ, deg	111.99 (3)	102.62 (3)
Z	2	2
V, $Å^3$	869.9	1471.9
d_{calcd}, g cm^{-3}	1.40	1.29
range of data coll (h, k, l)	(0, −11, −16) (11, 11, 16)	(0, −19, −13) (14, 18, 12)
no. of data coll	4246	7098
no. of unique data used	3232	4315
criteria for inclusion	$F_o > 3\sigma(F_o)$	$F_o > 3\sigma(F_o)$
temp, K	297 (1)	297 (1)
μ(Mo Kα), cm^{-1}	11.0	7.2
no. of parameters varied	190	325
2θ range, deg	3–55	3–55
abs corr range of trans coeff	empirical 0.94–1.0	empirical 0.98–1.0
R	0.058	0.056
R_w	0.091	0.070
highest peak of residual electron density, e/Å^3	0.6 (1)	0.53 (8)

[a] Numbers in brackets are estimated standard deviations in the least significant digits.

depend greatly on the solvent (see Table III), which excludes a photoelectrocatalytically process.

However, **2** is not the ultimate reaction product of photolysis with visible light. In the presence of PPh_3 **2** is inert, but photolysis in the presence of PPh_3 leads to the substitution of the last CO ligand according to eq 3 in 80% of isolated **3**.

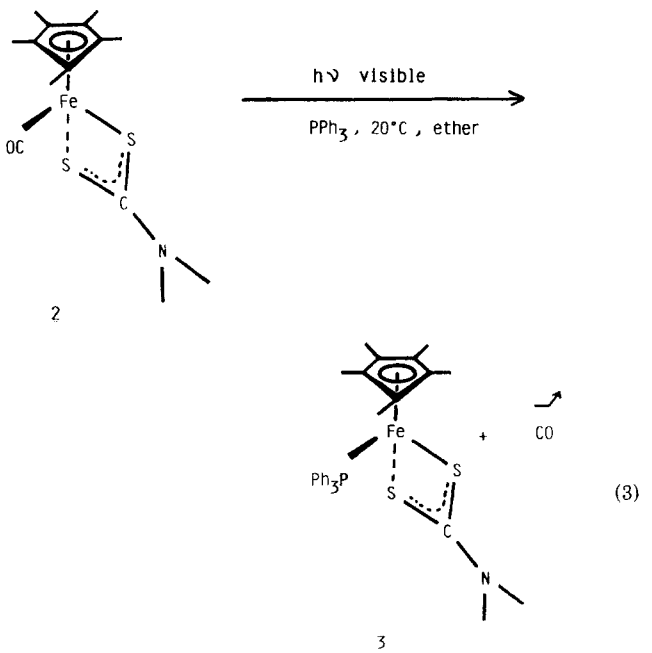

(7) Heller, G. H.; Langan, J. R. *J. Chem. Soc., Perkin Trans. 2* **1981**, 341.

Table V. Significant Interatomic Distances (angstroms) in Complex 1[a]

at. 1	at. 2	dist	at. 1	at. 2	dist
Fe	S1	2.271 (2)	N	C4	1.482 (9)
Fe	C1	1.772 (7)	N	C5	1.482 (9)
Fe	C2	1.771 (7)	C6	C7	1.429 (9)
Fe	C6	2.108 (6)	C6	C10	1.410 (9)
Fe	C7	2.101 (7)	C6	C61	1.52 (1)
Fe	C8	2.091 (7)	C7	C8	1.42 (1)
Fe	C9	2.106 (6)	C7	C71	1.50 (1)
Fe	C10	2.146 (5)	C8	C9	1.436 (9)
S1	C3	1.755 (5)	C8	C81	1.52 (1)
S2	C3	1.673 (5)	C9	C10	1.44 (1)
O1	C1	1.141 (9)	C9	C91	1.50 (1)
O2	C2	1.14 (1)	C10	C101	1.523 (9)
N	C3	1.344 (9)			

[a] Numbers in brackets are estimated standard deviations in the least significant digits.

Table VI. Significant Intramolecular Angles (degrees) in Complex 1[a]

at. 1	at. 2	at. 3	angle
S1	Fe	C1	93.9 (3)
S1	Fe	C2	92.1 (3)
S1	Fe	C6	106.8 (2)
S1	Fe	C7	146.5 (2)
S1	Fe	C8	143.6 (2)
S1	Fe	C9	103.7 (2)
S1	Fe	C10	86.5 (2)
C1	Fe	C2	97.7 (3)
Fe	S1	C3	113.4 (2)
C3	N	C4	120.8 (5)
C3	N	C5	123.5 (5)
C4	N	C5	115.7 (6)
Fe	C1	O1	172.5 (7)
Fe	C2	O2	172.3 (7)
S1	C3	S2	123.9 (4)
S1	C3	N	114.6 (1)
S2	C3	N	121.5 (4)
C7	C6	C10	108.8 (6)
C7	C6	C61	126.7 (6)
C6	C7	C8	107.0 (5)
C7	C8	C9	109.1 (6)
C8	C9	C10	106.4 (6)
C6	C10	C9	108.6 (5)

[a] Numbers in brackets are estimated standard deviations in the least significant digits.

Table VII. Significant Interatomic Distances (angstroms) in Complex 3[a]

at. 1	at. 2	dist	at. 1	at. 2	dist
Fe	S1	2.291 (2)	P	C21	1.848 (5)
Fe	S2	2.296 (1)	P	C31	1.866 (6)
Fe	P	2.224 (2)	N	C40	1.36 (1)
Fe	C1	2.114 (6)	N	C41	1.469 (8)
Fe	C2	2.100 (5)	N	C42	1.47 (1)
Fe	C3	2.093 (6)	C1	C2	1.43 (1)
Fe	C4	2.103 (6)	C1	C5	1.433 (8)
Fe	C5	2.101 (7)	C2	C3	1.432 (7)
S1	C40	1.708 (4)	C3	C4	1.435 (9)
S2	C40	1.704 (8)	C4	C5	1.432 (9)
P	C11	1.849 (5)			

[a] Numbers in brackets are estimated standard deviations in the least significant digits.

X-ray Crystal Structures of 1 and 3. The details of the X-ray crystal structure studies are summarized in Table IV, and significant bond distances and angles are given in Tables V–VIII. The X-ray crystal structure of **1** (Figure 2) confirms that the dtc ligand is bound to iron in the η^1 mode. The structural analysis of **3** shows the bulk around iron (Figure 3). Note that the Fe–S distance is significantly longer in **3** ((average 2.293 Å) than in **1** (2.271 Å).

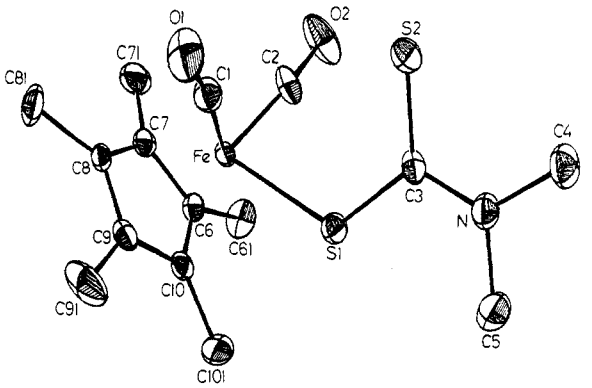

Figure 2. ORTEP view of the X-ray structure of complex 1.

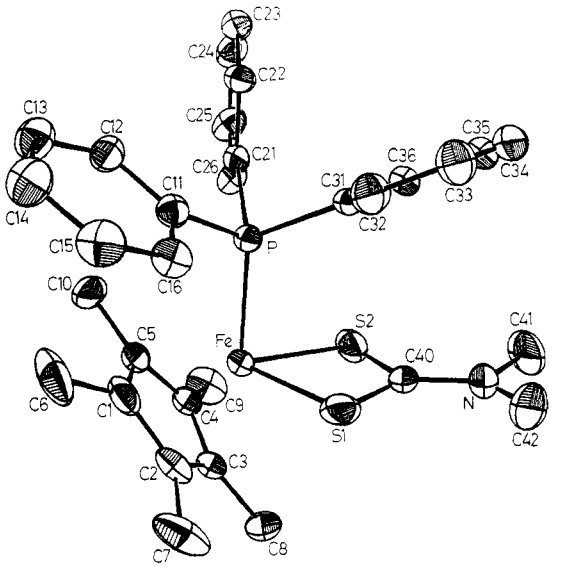

Figure 3. ORTEP view of the X-ray structure of complex 3.

Discussion

Comparison of the Photochemical and ET Reactions.[8] The photochemical chelation is a clean, facile, low-energy process. Usually, UV light is necessary for the photolytic removal of CO in neutral metal carbonyl complexes. The d–d transitions (ligand field (LF)) are responsible for most spectroscopic features of transition-metal complexes,[9a] which is also true for the piano stool compounds $FeCp(CO)_2X$.[9b] These photolytic d–d transitions usually provoke dissociative carbonyl loss because the photoexcited state has a strongly antibonding metal–carbonyl character.[9c] Occasionally, metal-to-ligand charge-transfer (MLCT) bands are found when the ligand has a low-lying antibonding orbital. In such cases, the photoexcited state is polarized M^+-L^-. Dissociative CO loss is then no longer obtained.[9c] Instead, the cationic metal center is much more susceptible to nucleophilic attack by incoming ligands, and associative CO exchange by nucleophiles is observed. However, such transitions are characterized by large extinction coefficients ($\epsilon = 10^3$–10^4 L mol^{-1} cm^{-1}) and sensitivity to the nature of the solvent.[9c] Although ϵ is large for 1, it is not in the MLCT range, and the sensitivity to solvents is weak. The blue shift observed from nonpolar to polar solvents indicates a stabilization of 5 kcal mol^{-1} of the HOMO in CH_3CN. Fluorescence, which gives indications about the excited state, was not found. However, a strong red shift is observed for 1 as compared to $FeCp(CO)_2Me$ ($\lambda = 356$ nm, $\epsilon = 1210$ L mol^{-1} cm^{-1} in CH_2Cl_2) and the ϵ value is considerably larger. Presumably, the LUMO of 1 is very covalent, i.e., it has both significant metal and ligand (dtc) character. If such is the case, then the transition would be accompanied by a significant polarization $Fe^{\delta+}$–$dtc^{\delta-}$ and the transition would be intermediate between LF and MLCT. This is still very favorable for nucleophilic attack of the free sulfur onto a positively charged iron center. However, no firm conclusion can be established concerning the associative or dissociative nature of the mechanism of Fe–CO cleavage.

A similar feature was encountered upon one-electron oxidation of complex 1. The ultrafast scanning of the cyclic voltammograms of 1 (up to 5000 V s^{-1}) performed by Verpeaux and Amatore[3] was unsuccessful in showing any character of reversibility upon anodic oxidation of 1. Thus 1^+ had a lifetime too short to be characterized by this technique. It is known that the general mechanism of ligand substitution in 17-electron complexes is associative and that such an exchange is 10^6–10^{10} times faster than in 18-electron complexes.[10] Here, the rate would still be greatly increased by the proximity of the incoming sulfur ligand. A major question raised in this study is whether photolytic chelation proceeds according to an electrocatalytic mechanism such as the redox-catalyzed thermal process. The value of the quantum yields ($\phi \simeq 0.6$) does not exclude a photoelectrocatalytic process with a low catalytic efficiency. However, in the electrocatalytic processes, the organometallic radicals involved in the chain

Table VIII. Significant Intramolecular Angles (degrees) in Complex 3[a]

at. 1	at. 2	at. 3	angle
S1	Fe	S2	75.54 (7)
S1	Fe	P	91.31 (7)
S2	Fe	P	90.50 (6)
Fe	S1	C40	86.8 (3)
Fe	S2	C40	86.7 (2)
Fe	P	C11	113.4 (2)
Fe	P	C21	120.2 (2)
Fe	P	C31	118.2 (2)
C11	P	C21	102.5 (2)
C11	P	C31	103.5 (2)
C21	P	C31	96.1 (2)
C10	N	C41	119.8 (8)
C40	N	C42	119.0 (5)
C41	N	C42	121.0 (8)
C2	C1	C5	107.9 (5)
C1	C2	C3	108.1 (5)
C2	C3	C4	107.9 (6)
C3	C4	C5	107.9 (4)
C1	C5	C4	108.1 (6)
P	C11	C12	122.0 (3)
P	C11	C16	117.7 (5)
P	C21	C22	119.9 (4)
P	C21	C26	119.6 (5)
P	C31	C32	123.1 (3)
P	C31	C36	116.4 (4)
S1	C40	S2	110.9 (4)
S1	C40	N	123.8 (5)
S2	C10	N	125.3 (4)

[a] Numbers in brackets are estimated standard deviations in the least significant digits.

(8) Desbois, M.-H.; Astruc, D. *Angew. Chem., Int. Ed. Engl.* **1989**, *28*, 460.

(9) (a) Geoffroy, G.; Wrighton, M. S. *Photochemistry of Organometallic Complexes*; Wiley: New York, 1983. (b) Alway, D. G.; Barnett, K. W. *Adv. Chem. Ser.* **1978**, *168*, 115. (c) Ferraudi, G. J. *Elements of Inorganic Photochemistry*; Wiley: New York, 1988; Chapters 5–7.

(10) (a) Poë, A. *Trans. Met. Chem.* **1982**, *7*, 65. (b) Trogler, W. C. *Int. J. Chem. Kinet.* **1987**, *19*, 1025. (c) Kochi, J. K. *J. Organomet. Chem.* **1986**, *300*, 19. (d) Baird, M. C. *Chem. Rev.* **1988**, *88*, 1217. (e) Astruc, D. *Chem. Rev.* **1988**, *88*, 1189.

are charged. The formation of such charged iron species would involve heterolytic cleavage of a metal–ligand bond induced by light. In such a case, the photocatalytic process responsible for the formation of charged species would be a charge transfer (metal-to-ligand or ligand-to-metal). The quantum yield would then depend very much on the polarity of the solvent, which is not the case (see Table III).

If the photolytic reaction gives better results than the electrocatalytic ones, it is not so if stoichiometric oxidation is used.[8] In the latter case, the yield is also quantitative for the production of 2^+ (eq 5) as well as for the synthesis of 3^+ in the presence of PPh_3 (eq 6). Similarly, 2^+ is rapidly and quantitatively converted into 3^+ by reaction with PPh_3 in various solvents (eq 7).[8]

$$1 \xrightarrow{\pm e^-} 2 \tag{4}$$

$$1 + [FeCp_2]^+PF_6^- \rightarrow 2^+PF_6^- + FeCp_2 \tag{5}$$

$$1 + [FeCp_2]^+PF_6^- + PPh_3 \rightarrow 3^+PF_6^- + FeCp_2 + CO \tag{6}$$

$$2^+PF_6^- + PPh_3 \rightarrow 3^+PF_6^- + CO \tag{7}$$

The facile photosubstitution of the second CO ligand (eq 3) suggests similar mechanistic considerations. Usually, the last carbonyl ligand is almost impossible to remove by using ultraviolet light. For instance, neither photolysis nor oxidation of $FeCp^*(CO)(\eta^1\text{-dppe})(CH_3)$ displaces CO by the pendent P ligand, probably because there is no low-lying ligand π^* orbital in dppe.[11] In the case of the photolysis of **2** (eq 3), visible light is efficient as is oxidatively induced ligand exchange. The case of oxidation of **2** and other analogous dtc complexes is related to the ability of the dtc ligand to stabilize high oxidation states.[1] This trend is attributable to the electron-reservoir property of the transition metal–η^2-dtc framework, a delocalized system with two polarizable electron-rich sulfur atoms transferring electron density from the N atom:

Synthetically, both the photochemical and ET routes are convenient for the synthesis of $2/2^+$ and $3/3^+$. The redox reagents $[FeCp_2]^+PF_6^-$ and $Fe^ICp(HMB)$ easily interconvert the cationic and neutral form in high yields (eq 8).[6c,8,12]

$$\underset{18e}{2 \text{ (or } 3)} \underset{Fe^ICp(HMB)}{\overset{[Fe^{III}Cp_2]^+PF_6^-}{\rightleftharpoons}} \underset{17e}{2^+PF_6^- \text{ (or } 3^+PF_6^-)} \tag{8}$$

Comparative Bulk from the X-ray Crystal Structures of 1 and 3. Note that the 17-electron complex 3^+ is stable at 20 °C whereas the 17-electron complex 1^+ is so transient that it cannot be observed even by using fast-scan cyclic voltammetry. The crystal structures of their precursors **1** and **3** recorded here can be compared in this respect. That of **1** shows that the iron center is readily accessible for the attack by the free sulfur of the monodentate dtc ligand, one side of the coordination sphere being widely open (Figure 2). That of **3** shows that the iron center is sterically crowded by the three bulky ligands η^5-Cp*, η^2-dtc, and PPh_3 (Figure 3). Under these conditions, the classical associative mechanism for the ligand substitution in 17-electron complexes is no longer accessible for 3^+ and only the dissociative mode will be operative. This latter mode leads to an Fe^{IV} complex and is discussed elsewhere.

Experimental Section

General Procedures. Reagent grade diethyl ether and pentane were predried over Na foil and distilled from sodium benzophenone ketyl under argon just before use. Methylene chloride was distilled from calcium hydride just before use. All other chemicals were used as received. All manipulations were done by Schlenk technique or in a nitrogen-filled Vacuum Atmospheres drylab. Electronic spectra (UV and visible) were recorded with a Cary 219 spectrophotometer with 10-mm quartz cells modified for work with air-sensitive compounds. Solutions (10^{-4} mol/L) of the desired complex were prepared in the dark, under argon, and then exposed to a 1000-W Xe lamp with a monochromatic wavelength selector (λ = 330 nm), for selected times. The evolution of the reaction was monitored by visible spectroscopy. (*E*)-α-(2,5-Dimethyl-3-furylethylidene)(isopropylidene)succinic anhydride was used as chemical actinometer,[7] to estimate the radiant flux. $[FeCp^*(\eta^1\text{-dtc})(CO)_2]$ was obtained according to the literature.[5] X-ray crystals were grown by slow recrystallization at −20 °C of a saturated solution of the complex in ether. $[FeCp^*(\eta^2\text{-dtc})(PPh_3)]$ was obtained by slow recrystallization, at −20 °C, of a saturated solution of the complex in pentane.

X-ray Analyses. A summary of the crystal data collection and structure refinement is given in Table IV. Suitable crystals of **1** and **3** were chosen and placed on an Enraf-Nonius CAD-4 diffractometer. The parameters were refined, in both cases, for 25 reflections in the range $28 < 2\theta < 32°$ by using graphite monochromated Mo Kα X radiation. Data were collected at 297 (1) K, by using the θ–2θ scan mode, variable scan rate 2–10°/min, in ω with scan width = 0.8 + 0.35 tan θ. Two standard reflections were measured after every 3600 s of X-ray exposure, and two orientation standards after every 100 reflections collected, with a recalculation of the orientation of the matrix after any significant angular deviation.

For both **1** and **3**, the centrosymmetric triclinic space group gave successful structure refinement. The structures were solved by Patterson and difference syntheses, with full-matrix least-squares refinement of *F*. All atoms were anisotropically refined (data/parameter ratio = 17.0 (**1**), 13.3 (**3**)). A weighting scheme was incorporated into the refinement with $w = 4F_o^2/(\sigma_{count} + (0.04F_o^2)^2)$ for **1** and $w = 4F_o^2/(\sigma_{count} + (0.04F_o^2)^2)$ for **3**. All computations were carried out using a VAX computer with Enraf-Nonius SDP/VAX programs.[13] Scattering factors including f' and f'' were taken from ref 14.

Preparations. Determination of Radiant Flux. An accurately measured volume (*V*) of a solution of actinometer in toluene at a concentration sufficient to absorb all the incident radiation is exposed to UV light (λ = 330 nm) for 10 s, and the increase in absorbance (ΔA) at 494 nm is the maximum of the long-wavelength band of the product of transformation. The radiant flux (*I*) is calculated from the expression $I = AVN/\phi\epsilon t$ photons s^{-1}, where *N* is the Avogadro number 6.023×10^2 mol^{-1}, ϕ is the quantum yield for photocoloration (0.20 for irradiation at 330 nm), ϵ is the molar extinction coefficient of the 7,7a-dihydro-2,4,7,7a-pentamethylbenzo[*b*]furan-5,6-dicarboxylic anhydride (8200 at 494 nm), and *t* the irradiation time (10 s). The calculated radiant flux (1.042×10^{16} photons/s) was used to obtain the quantum yield of the chelation. Short irradiation times (10 s) were used because of the absorption of both complexes in the 330-nm region (see Table II for results).

$FeCp^*(\eta^2\text{-dtc})(CO)$ (2). A 0.100-g sample of complex **1** (0.272 mmol) in 5 mL of CH_2Cl_2 was photolyzed (visible light) under argon, at room temperature. The reaction followed by infrared spectroscopy took 1 h, CH_2Cl_2 was removed in vacuo and the crude

(11) Morrow, J.; Catheline, D.; Desbois, M.-H.; Manriquez, J.-M.; Ruiz, J.; Astruc, D. *Organometallics* **1987**, *6*, 2605, and unpublished observations.
(12) Astruc, D. *Acc. Chem. Res.* **1986**, *19*, 377.
(13) Enraf-Nonius (1984); Structure Determination Package; Enraf-Nonius, Delft, The Netherlands.
(14) *International Tables for X-ray Crystallography*; Kynoch Press: Birmingham, England, 1974; Vol IV (present distributor Kluwer Academic Publishers, Dordrecht).

product extracted with pentane. Concentration of the solvent and recrystallization gave 0.090 g (94% yield) of complex **2** identified by comparison with an authentic sample.[2]

FeCp*(η^2-dtc)(PPh_3) (3). A 0.100-g sample of complex **2** (0.295 mmol) and 0.077 g of PPh_3 (0.295 mmol) in 5 mL of ether were photolyzed (visible light) under argon, at room temperature. The reaction followed by IR spectroscopy took 1 h. Ether was removed in vacuo, and the crude product extracted with pentane. Concentration of the solvent and recrystallization gave 0.125 g (80% yield) of complex **3** identified by comparison with an authentic sample.

Acknowledgment. We thank Dr. R. Lapouyade (Université de Bordeaux I) for his kind help in recording photochemical experiments and for very pertinent discussions. The Centre National de la Recherche Scientifique, the University of Bordeaux, the Conseil Régional d'Aquitaine, the National Science Foundation, and the Robert A. Welch Foundation are gratefully acknowledged for financial support.

Registry No. 1, 89875-07-0; 2, 84541-24-2; 3, 119366-44-8.

Supplementary Material Available: Tables of anisotropic thermal parameters of non-hydrogen atoms for complexes 1 and 3 (31 pages); listings of the observed and calculated structure factors for 1 and 3 (32 pages). Ordering information is given on any current masthead page.

Systematic Synthesis, Solution Structural Characterization of the Square-Pyramidal Clusters $MIr_4(CO)_7(\mu\text{-}CO)_2L(\eta^5\text{-}C_5Me_5)(\mu_4\text{-}PPh)$ (M = Rh, Ir; L = CO, PPh_3), and X-ray Structural Determination of the Iridium Derivatives

Rajesh Khattar,[1a] Stephen Naylor,[1b] and Maria D. Vargas*,[1c]

University Chemical Laboratory, Lensfield Road, Cambridge CB2 1EW, U.K.

Dario Braga* and Fabrizia Grepioni

Dipartimento di Chimica "G. Ciamician", Università degli Studi di Bologna, Via Selmi 2, 40126 Bologna, Italy

Received June 23, 1989

The pentanuclear clusters $MIr_4(CO)_9L(\eta^5\text{-}C_5Me_5)(\mu_4\text{-}PPh)$ [L = CO, M = Rh (**3**), Ir (**4**) and L = PPh_2Me or PPh_3, M = Rh (**3a**) or (**3b**), Ir (**4a**) or (**4b**)] are synthesized in good yields by the reactions of $Ir_4(CO)_{11}(PPhH_2)$ and $Ir_4(CO)_{10}(PPhH_2)L$ (L = PPh_2Me or PPh_3), respectively, in acetonitrile with $[M(\eta^5\text{-}C_5Me_5)(NCMe)_3][SbF_6]_2$ (M = Rh, Ir) in the presence of 1,8-diazabicyclo[5.4.0]undec-7-ene (DBU). Compounds **3a**, **3b**, **4a**, and **4b** are also obtained by the reactions of **3** and **4**, respectively, either with L (L = PPh_2Me or PPh_3) in the presence of Me_3NO or with Bu_4NBr to give $[MIr_4(CO)_9Br(\eta^5\text{-}C_5Me_5)(\mu_4\text{-}PPh)]^-$, followed by bromide abstraction with $AgSbF_6$ in the presence of L. All compounds are characterized by fast-atom bombardment mass spectrometry and a combination of ^1H, ^{13}C and ^{31}P NMR. The solid-state structures of **4** and **4b** show that the phosphinidene ligand μ_4 bridges the square base of the square-pyramidal metal atom framework, while the C_5Me_5 is coordinated to one basal Ir atom. The PPh_3 ligand in **4b** replaces an axial CO opposite to the C_5Me_5 group with respect to **4**. Crystal data for **4**: space group $P\bar{1}$, a = 14.511 (5), b = 15.366 (8), c = 13.962 (2) Å, α = 89.99 (3), β = 93.94 (2), γ = 86.15 (3)°, Z = 4. Crystal data for **4b**: space group $P2_1/a$, a = 17.949 (2), b = 9.998 (4), c = 25.606 (5) Å, β = 108.94 (1)°, Z = 4. The solution structures of **3**, **4**, **3b**, and **4b** were determined by low-temperature ^{13}C NMR and are fully consistent with the solid-state structures. For the isostructural compounds **3** and **4** two separate averaging processes are observed at higher temperatures, the first of which has been explained in terms of the formation of the ground-state structure mirror image, complete averaging of all carbonyls occurs at room temperature in these species and also in **3b** and **4b**, whose ^{13}C NMR data did not yield any further mechanistic information.

Introduction

A number of metal carbonyl clusters stabilized by phosphinidene (PR) ligands have been reported during the past few years.[2] Skillfull preparative routes to a range of trinuclear species containing one or even two μ_3-PR ligands have been established;[3] studies of their reactivity have contributed significantly to a better understanding of ligand addition and substitution reactions of metal carbonyl clusters.[4] Recent comparative studies of the reactivity of a number of bis-μ_4-PR square-planar tetranuclear clusters of both the cobalt and iron subgroups could be achieved only as a result of the development of reliable synthetic routes.[5] Such studies have not yet been extended to phosphinidene clusters of nuclearity higher than four, as their isolation has mostly been the result of ser-

(1) Present address: (a) Department of Chemistry and Biochemistry, University of California, Los Angeles, CA 90024; (b) MRC Toxicology Institute, Carshalton, Surrey SM5 4EF, England. (c) Instituto de Quimica, Universidade Estadual de Campinas, C.P. 6154, Campinas 13081, SP, Brazil.

(2) Huttner, G.; Knoll, K. *Angew. Chem., Int. Ed. Engl.* **1987**, *26*, 743.

(3) Huttner, G.; Schneider, J.; Müller, H. D.; Mohr, G.; von Seyerl, J.; Wohlfart, L. *Angew. Chem., Int. Ed. Engl.* **1979**, *18*, 76.

(4) Lunniss, J.; Mac Laughlin, S. A.; Taylor, N. J.; Carty, A. J.; Sappa, E. *Organometallics* **1985**, *4*, 2066.

(5) (a) Vahrenkamp, H.; Wucherer, E. J.; Walter, D. *Chem. Ber.* **1983**, 116, 1219. (b) Müller, E. J. *Angew. Chem., Int. Ed. Engl.* **1981**, *20*, 680.

0276-7333/90/2309-0645$02.50/0